Nuclear Instruments and Methods in Physics Research A 833 (2016) 142–148

Contents lists available at ScienceDirect

Nuclear Instruments and Methods in Physics Research A

journal homepage: www.elsevier.com/locate/nima

LISe pixel detector for neutron imaging

Elan Herrera [a], Daniel Hamm [a], Brenden Wiggins [b,c], Rob Milburn [a], Arnold Burger [c,d], Hassina Bilheux [e], Louis Santodonato [f], Ondrej Chvala [a], Ashley Stowe [a,b,c], Eric Lukosi [a,*]

[a] Department of Nuclear Engineering, University of Tennessee, Knoxville, TN, USA
[b] Technology Development, Y-12 National Security Complex, Oak Ridge, TN, USA
[c] Department of Physics and Astronomy, Vanderbilt University, Nashville, TN, USA
[d] Department of Life and Physical Sciences, Fisk University, Nashville, TN, USA
[e] Chemical and Engineering Materials Division, Oak Ridge National Laboratory, Oak Ridge, TN, USA
[f] Instrument and Source Division, Oak Ridge National Laboratory, Oak Ridge National Laboratory, Oak Ridge, TN, USA

ARTICLE INFO

Article history:
Received 12 October 2015
Received in revised form
11 July 2016
Accepted 16 July 2016
Available online 18 July 2016

Keywords:
$^{6}LiInSe_2$
LISe
Neutron detection
Neutron imaging
Pixel detector
Semiconductor detector

ABSTRACT

Semiconducting lithium indium diselenide, $^{6}LiInSe_2$ or LISe, has promising characteristics for neutron detection applications. The 95% isotopic enrichment of ^{6}Li results in a highly efficient thermal neutron-sensitive material. In this study, we report on a proof-of-principle investigation of a semiconducting LISe pixel detector to demonstrate its potential as an efficient neutron imager. The LISe pixel detector had a 4×4 of pixels with a 550 μm pitch on a $5 \times 5 \times 0.56$ mm^3 LISe substrate. An experimentally verified spatial resolution of 300 μm was observed utilizing a super-sampling technique.

1. Introduction

Cold neutron radiography and tomography comprise powerful detection tools for investigating both natural and engineered materials. Its sensitivity for real-space imaging relies on the total neutron interaction cross section with the material under investigation, which includes both scattering (neutron-nuclei and neutron-lattice) and absorption [1]. Neutron imaging shares many similarities with X-ray imaging systems, albeit the mode of interaction of the interrogating beam is different. The comparison between these two imaging techniques is outside the scope of this study, but many references are available [1–3].

In the advancement of the capabilities of neutron imaging facilities, it has been indicated that there is a need for advances in suitable detection systems to reach the full potential of current and future neutron facilities, such as the Spallation Neutron Source (SNS) at Oak Ridge National Laboratory (ORNL). Specifically, a simultaneous enhancement of the detection efficiency (ideally 100%), spatial resolution (less than 10 μm), large signal-to-noise ratio, (good gamma-ray rejection capability), and high temporal resolution (less than 1 μs) is desired [4]. Achieving the desired performance metrics outlined is a challenging prospect, but the use of a semiconductor-based imaging plane may provide the necessary performance.

Current semiconductor-based cold neutron imagers rely on the use of a converter layer on a semiconductor detector [1,5,6]. The converter material is enriched with an isotope exhibiting large neutron capture cross section at thermal/cold energies, commonly ^{6}Li, ^{10}B or ^{157}Gd. The range of secondary charged particles in the converter layer, however, result in a few percent detection efficiency for thermal neutrons using ^{10}B and ^{6}LiF converter layers [7]. Further, transport of energetic charged particles may result in a decreased energy resolution [5,6]. Using ^{157}Gd or ^{113}Cd, which both have neutron capture cross sections an order of magnitude or more than ^{10}B and ^{6}Li, can result in efficiencies up to 40% [8]. Further, Gd- and Cd-based detection systems have the potential for high-resolution imaging because of the lower energy and range of the emitted particles in the neutron reaction compared to ^{6}Li and ^{10}B, limited only by the pixel density and pitch of the sensing substrate. However, the low energy of conversion electrons and x-rays emitted from ^{nat}Gd and ^{113}Cd results in a poor signal-to-noise ratio and are subject to image contamination from internal and external gamma-rays. Imaging contamination from gamma-rays using ^{10}B and ^{6}LiF coated sensors is also an issue, where higher thresholds may be required to minimize image contamination, resulting in reduced detection efficiency [5,6]. Therefore, although neutron imaging systems using semiconductors

* Corresponding author.
E-mail address: elukosi@utk.edu (E. Lukosi).

http://dx.doi.org/10.1016/j.nima.2016.07.035
0168-9002/

have been investigated, the low efficiency and/or poor signal-to-noise ratio have commonly led to the use of other types of detection systems, which have their own limitations of the achievable spatial resolution, neutron detection efficiency, and temporal resolution. For further discussion on different types of neutron imaging systems, the reader is referred to these excellent references [1,3,9–12].

Lithium indium diselenide (^{6}LiInSe$_2$ or LISe) is a relatively new $A^{I}B^{III}X_2^{VI}$ type semiconductor with a band gap of 2.8 eV [13]. It possesses a 24% ^{6}Li concentration within the regular stoichiometry of the crystal, eliminating the need for separated conversion and detection layers. The detection of neutrons by LISe relies on the ^{6}Li(n,^{3}H)^{4}He reaction, and the large 4.78 MeV Q-value of the reaction provides an intrinsic potential for excellent neutron/gamma discrimination. The mean free path of thermal neutrons in LISe is 920 μm, enabling the use of thin LISe substrates for potentially efficient neutron detection. With these attributes, LISe may provide the desired sensor system attributes previously outlined. This report presents on the development and evaluation of a proof-of-principle LISe pixel detector to investigate its potential for cold neutron radiography.

2. Materials and methods

2.1. Neutron imaging sensor development

The LISe pixel detector was prepared by the synthesis method of Tupitsyn et al. [13] using lithium enriched in ^{6}Li to 95 at%. A $5 \times 5 \times 0.56$ mm^3 yellow LISe crystal was used as the sensor substrate because they typically exhibit the best semiconducting properties (see Fig. 1) [14]. Substrate processing and LISe pixel detector fabrication took place at the Micro-Processing Research Facility at the University of Tennessee [15]. A 4×4 pixel pattern with a pitch of 550 μm and a 100 μm guard ring was deposited on the LISe sensor substrate using negative liftoff photolithography, as shown in Fig. 2 [16]. Indium was deposited via RF magnetron sputtering. Following successful patterning, the pixelated LISe sensor substrate (LISe pixel detector) was mounted to a custom sensor board using electronic grade silver paste and gold wire wedge bonding (see Fig. 3) [17].

The front-end electronics was designed using CadSoft EAGLE PCB Design Software™. The preamplifier circuit consists of twin 8-channel boards, where each board has its own filtered high-voltage line to bias the LISe pixel detector. Each pixel, or channel, from the sensor board was AC-coupled to Cremat® CR-110 (rev. 2) charge sensitive preamplifiers. A central DC power supply powered the 16 Cremat CR-110 (rev. 2) preamplifiers through isolated +12 V and −12 V bias lines with respect to earth ground. The imaging system operates at room temperature and no cooling systems were utilized for the LISe pixel detector or the front-end electronics. A single extruded aluminum enclosure encased the sensor board and front-end electronics, serving as an EMI and light shield. Aluminum is relatively transparent to cold neutrons, limiting neutron scattering and subsequent image degradation. The completed LISe pixel detector with the lid of the aluminum enclosure removed is presented in Fig. 3.

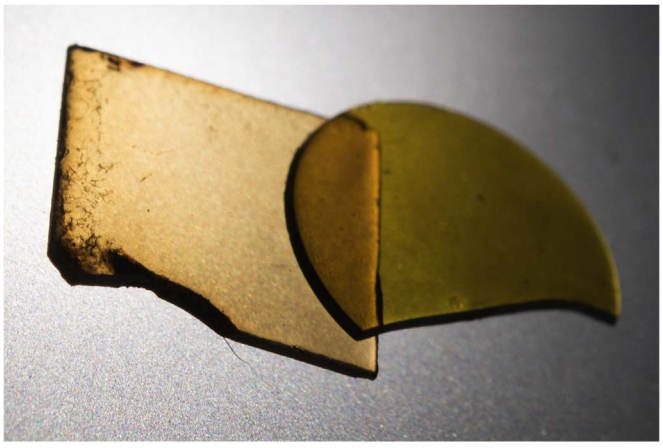

Fig. 1. Two semiconducting LISe crystals (~7 mm largest dimension).

2.2. Experimental

The developed LISe pixel detector was tested at the High-Flux Isotope Reactor (HFIR) CG-1D Neutron Imaging Beamline at ORNL. The beam line exhibits an average neutron flux of $\sim 7 \times 10^6$ n/cm^2/s between 0.8 Å and 6 Å with a peak at ~2.6 Å at the beam port [18,19]. The distance from the installed ZnS:^{6}LiF imaging plane and the point aperture used for these measurements was 6.6 m [20]. The LISe pixel detector was suspended on an aluminum extrusion approximately 0.3 m in front of the ZnS:^{6}LiF scintillation screen (see Fig. 4).

Digital signal processing was carried out using two CAEN V1724 8-Channel Digitizers with on-board DPP-PHA processing interfaced to a PC via the A3818 PCI Express CONET2 Controller and CAEN V2718 bridge. The LISe pixel detector was biased at 250 V using a NHQ 203M Dual High Voltage Power Supply housed separately in an ORTEC 4001C NIM bin crate.

A 3/8 in. stainless steel bolt and PSI Siemens Star test pattern were used to test the LISe pixel detector [21]. The purpose of the bolt test was to image the thread pattern. The PSI mask has an outer diameter of 20 mm with 128 Gd spokes (line/space pairs). From the innermost radius outwards, concentric rings provide visual pitch resolution markers between 40 μm and 500 μm. A motorized stage was used to image objects larger than the 2.2×2.2 mm^2 active area of the LISe pixel detector via translation in the plane perpendicular to the cold neutron beam.

The LISe pixel detector was positioned along the centerline of the cold neutron beam where the flux approaches a maximum and is most uniform [19,20]. A custom LabVIEW™ program was created to automate bolt or PSI mask translation and data collection, where the measurement and translation stage movement times can be independently set to optimize exposure time and required sample translation time. This level of control allowed PSI mask translation below the pixel pitch of the LISe pixel sensor, now called the super-sampling technique, where the resolution of the LISe pixel detector is enhanced beyond the pixel pitch via data analysis techniques, as described in Section 2.4. In Fig. 5, an image of the PSI mask and the range of positions investigated with the LISe pixel detector relative to the mask is provided. Here, the translation stage in the imaging sweep moved the PSI mask with a step size of 125 μm along 22 steps on both axes. A ten-second measurement time was used at each position with a two second movement time between measurement points.

2.3. Simulation

The experimental evaluation of the LISe pixel detector with the PSI mask was simulated to provide a benchmark for the experiment and provide an expected performance metric of the super-sampling technique. MCNP6 [22] was used to investigate a 4×4 LISe pixel detector with a pitch of 900 μm. The distance between the LISe pixel detector and the PSI mask was 15 cm. The plane wave neutron source was emitted from a circular surface with a 5 cm radius at 25 meV with zero divergence. Each simulation transported 10^9 neutrons. The point spread function of the LISe